Supplementary Information for

Magnet Patterned Superparamagnetic Fe_3O_4/Au Core-Shell Nanoplasmonic Sensing Array for Label-Free High Throughput Cytokine Immunoassay

Yuxin Cai[†], Jingyi Zhu[‡], Jiacheng He[†], Yang Wen[†], Chao Ma[‡], Feng Xiong[§], Feng Li[§], Weiqiang Chen[‡], and Pengyu Chen[†,]*

[†] Materials Research and Education Center, Materials Engineering, Department of Mechanical Engineering, Auburn University, Auburn, AL, USA.

[‡] Department of Mechanical and Aerospace Engineering, New York University, New York, NY, USA.

§ Department of Drug Discovery and Development, Harrison School of Pharmacy, Auburn University, Auburn, AL, USA

[*]To whom correspondence should be addressed. E–mail: pengyuc@auburn.edu

1) **Characterization of Fe_3O_4/Au core-shell magnetic nanoparticles:** We synthesized the Fe_3O_4/Au core-shell magnetic nanoparticles (FACSNPs) using a modified one-pot solvothermal method. The CTAB coating on the FACSNPs resulted in a positively charged surface with a zeta potential of 46 ± 6 mV (Zetasizer Nano ZS90, Malvern). The transmission electron microscopy (TEM) was used to characterize the synthesized FACSNPs as shown in Fig. S1a. The dimensions of the FACSNPs and the decorated AuNPs were measured to be 60 ± 6 nm and 19 ± 2 nm, respectively (Fig. S1b). Fig. S1c the XRD results of the diffraction spectrum of Fe_3O_4 nanospheres (NS). The sharp diffraction peaks were indexed to be (112), (211), (202), (220), (312), (303), (224), (332) and (143) Bragg reflections of crystalline cubic inverse spinel of bulk Fe_3O_4, respectively (JCPDS no. 75-1609).

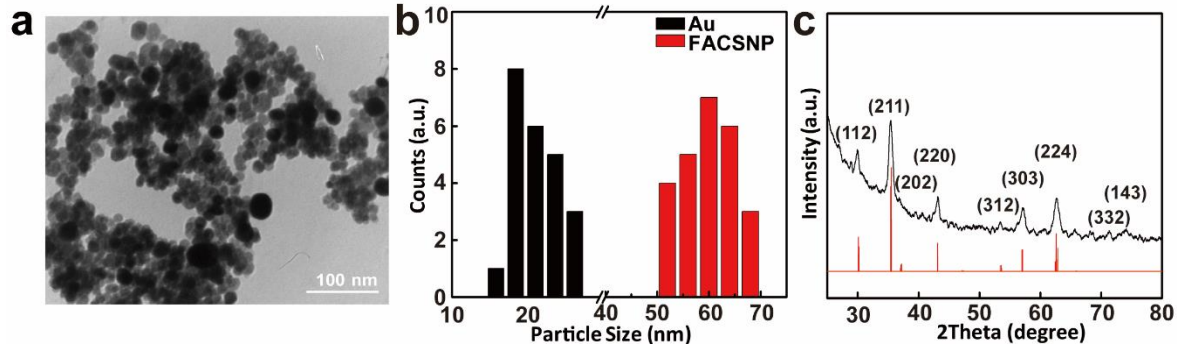

Figure S1. (a) Transmission electron microscopy of FACSNPs drop-cast onto a glass substrate. (b) Statistics size distributions of the embedded gold nanoparticles and the FACSNPs measured from a high magnification of the TEM in (a). (c) XRD spectrum of Fe_3O_4 NS. The red line is the standard XRD pattern of JCPDS no. 75-1609.

2) Electromagnetic-field optical simulation on a single FACSNP upon local refractive index change: We performed a finite difference time domain (FDTD) simulation and predicted the scattering efficiency on a single FACSNP. The optical response of FACSNPs upon light excitation was simulated by the finite element method using commercial multi-physics simulation software (COMSOL). The dimensions of Fe_3O_4 NS and the decorated AuNPs were determined based on

the TEM results in Fig. S1. The far-field domain was constructed as a semi-sphere and the perfectly matched layer with the same radius was set on the top of the far-field domain as the boundary of light. A polarized incident electromagnetic wave that was perpendicular to wave vector was set. The absorption light intensity was evaluated by the absorption cross section C_ACS, which is the integration of the absorption wave intensity over the surface of far-domain Ω.

$$C_{ACS} = \int \frac{I_{AuNP}}{I_{background}} d\Omega,$$

where I_{AuNP} is the absorbance intensity from the AuNPs and $I_{background}$ the background signal without the presence of AuNPs.

3) The superparamagnetism feature of the FACSNPs: Figure S2 shows the effect of an external magnetic field on the FACSNPs under a dark-field microscope. When an external magnetic field was applied, the FACSNPs can be magnetized and well aligned with the external magnetic field (Fig. S2a). The removal of the external magnetic field resulted in the immediate random dispersion of the FACSNPs (Fig.S2b). These observations are in consistent with the magnetism measurement of the hysteresis loops, confirming the superparamagnetism of the FACSNPs.

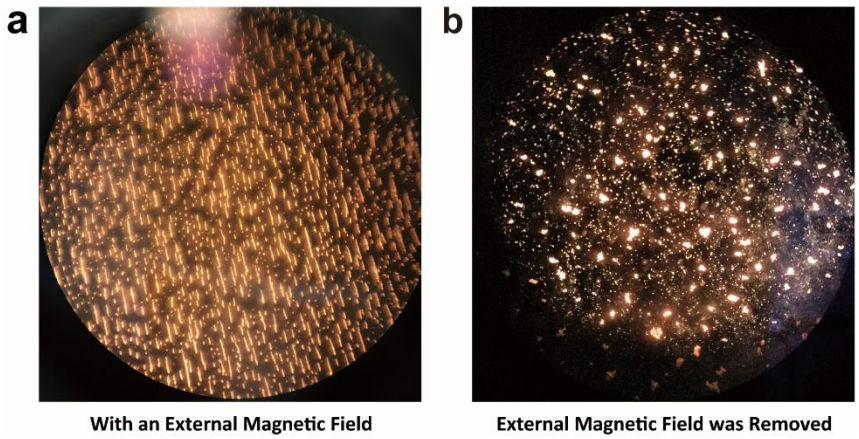

Figure S2. (a) Dark field image of the FACSNPs drop-cast into the center of a glass substrate with an external magnetic field. The FACSNPs spontaneously lined up with the orientation of the magnetic field lines. (b) Dark field image of the on-glass FACSNPs right after the external magnetic field was removed, the FACSNPs immediately redispersed in the aqueous solution.

4) FACSNP microarray fabrication: Prior to the FACSNPs microarray fabrication, we first prepared PDMS micro well mask layers in both square and round shapes using soft lithography. The mold for the PDMS well-patterning mask was fabricated on a silicon substrate using deep reactive-ion etching (DRIE). The PDMS prepolymer (Sylgard-184, Dow Corning) was prepared by thoroughly mixing a curing agent with a base monomer (wt : wt = 1 : 10) and poured onto the silicon mold and cured in an oven at 65°C for 6 hrs. The cured PDMS mask layer was then peeled off from the mold to form a well-patterning mask layer. The layer was cut into multiple pieces for future use.

In order to precisely deposit the FACSNP microarrays on desired positions of the chip, we designed a 3D-printed polylactic acid (PLA) mold. A substrate was mounted into the 3D-printed mold to assist the positioning of the PDMS masks later. Glass slides were first cleaned with Piranha solution (H_2SO_4:H_2O_2 = 3:1 v/v) for 10 min, rinsed thoroughly with deionized water, and kept in an ultrasonic bath with ethanol for 15 min. Then, the PDMS micro well-shape masks and a glass substrate were both treated with an oxygen plasma (Plasma Etch, Inc.) for 2 minutes. After plasma treating, the PDMS masks became hydrophilic and allowed the proper wetting of the FACSNPs aqueous dispersion on the masks. The plasma treated glass substrate turned to negatively charged owing to the dissociated hydroxyl groups existing on the glass, which can interact with the positively charged CTAB coated FACSNPs and immobilize them onto the surface. After that, the micro well-shape PDMS masks were mounted into the 3D-printed plastic mold. The plastic mold was detached after the PDMS mask positions were fixed. Each area of the plasma treated PDMS masks were filled with 3.5 μL of FACSNPs dispersion. Then, the whole device was degassed in a

vacuum desiccator for 25 min. The excessive FACSNP aqueous dispersion on the surface of the PDMS masks was removed after degassing. The plasma treated the glass substrate was then attached to the FACSNPs loaded PDMS microwell layer. Strong ceramic magnets were fixed on the other side of the glass substrate to attract the FACSNPs to the glass surface. The whole device was incubated in a humid environment overnight. After incubation, the magnet and the PDMS masks were removed. The fabrication processes were shown in detail in Fig.S3.

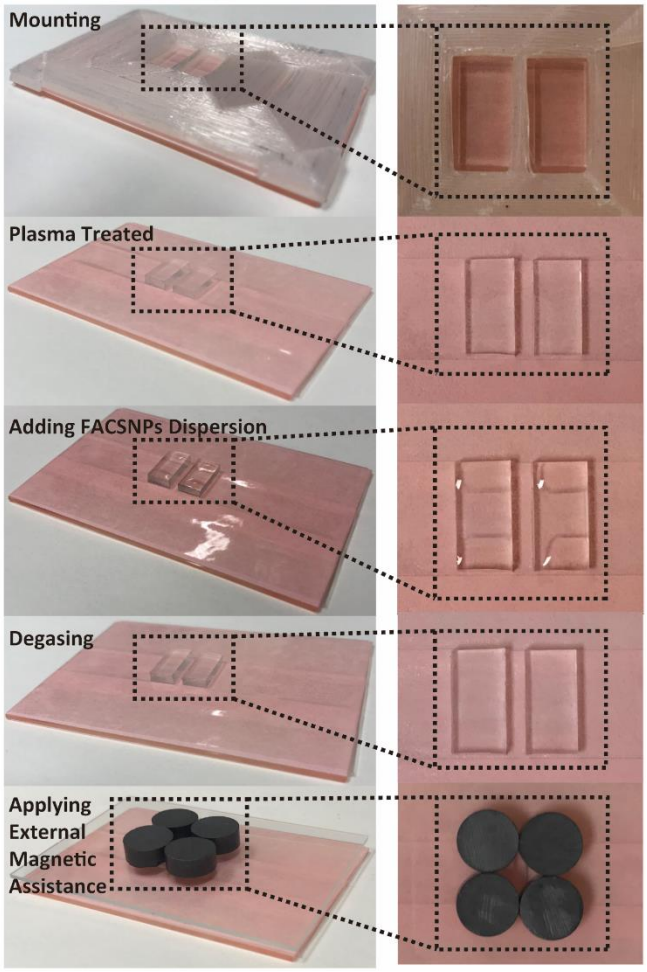

Figure S3. Photographs showing the detailed fabrication processes of the magnet assisted patterning of FACSNP microarray

We compared the patterning quality of the FACSNP microarray with and without the magnets as shown in Fig. S4a and Fig. S4b. The magnet assisted patterning of FACSNP microarray showed

clearly better uniformity on the shape and intensity of the array spot. Without the external magnetic field, aggregations, unfilled patterns and "coffee-ring" shapes of the FACsNPs were observed on the glass substrate after overnight incubation. PDMS masks with different dimensions and geometries of the micro wells were also used for creating different FACSNP microarray patterns. We obtained nicely patterned microarrays with square shape of 20 μm × 20 μm (spot-to-spot distance = 40 μm, main text Fig. 2c and Fig. S4a), mini square shape of 15 μm × 15 μm (spot-to-spot distance = 25 μm, Fig. S4c) and round shape of 40 μm in diameter (spot-to-spot distance = 60 μm, Fig. S4d). These results demonstrate the tunability and scalability of our magnet assisted patterning technique for FACSNP microarrays.

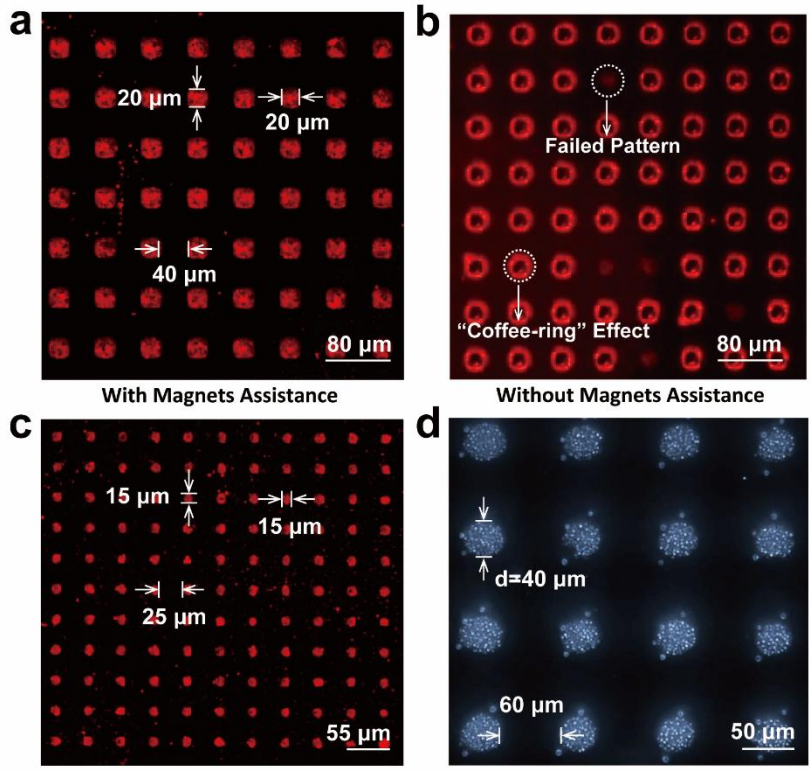

Figure S4. (a) Dark field image of the sensing spots pattern formed with magnets assistance. (b) Dark field image of the sensing spots pattern formed without magnets assistance. (c) Dark field image of mini square-shape biosensing spots arrays. (d) Dark field image of the round-shape patterned sensing spots, in which the FACSNPs dispersed uniformly.

5) Real-time Detection and Sensor Calibration: Figure S5a shows the real-time intensity increasing curves from one set of the FACSNP microarray (4 × 4) for detecting MCP-1 of 1000 pg/mL. We further obtained the calibration curves of IL-6, MCP-1, TNF-α and TGF-β based on the FACSNP microarray intensity increase in response to different concentrations of cytokine exposure (Fig. S5b). To validate the multiplex sample measurement capability of the microarray immunoassay that can specifically detect target cytokines in a complex biological medium, we performed measurements on a set of samples with each containing only one specific type of the cytokines (IL-6, MCP-1, TNF-α and TGF-β) at the concentration of 1000 pg/mL. As shown in Fig.

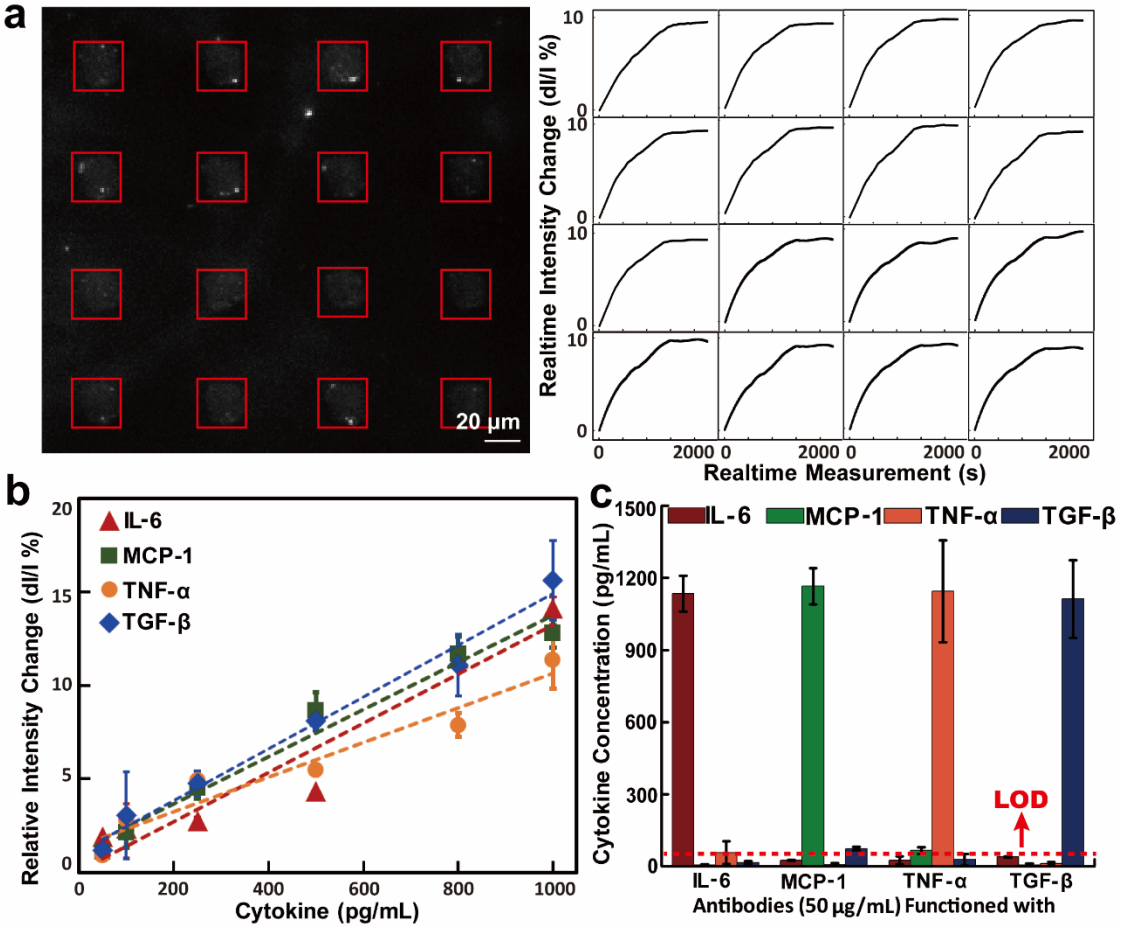

S5c, we found no statistically significant difference between the measured cytokine concentrations and their expected values of 1000 pg/mL. Furthermore, most of the sensors targeting cytokines absent in the mixture yielded signals below the limit of detection as anticipated.

Figure S5. (a) Real time binding curves of 16 FACSNP microarray sensing spots for detecting spiked MCP-1 of 1000 pg/mL. (b) Calibration curves of IL-6, MCP-1, TNF-α and TGF-β obtained from the FACSNP microarray immunoassay. (c) The selectivity of multiplex microarray immunoassay measured in cytokine concentrations. The red dash line is the limit of detection of our FACSNP microarray immunoassay. Data were presented as the mean ± SD (n= 3).

6) Correlation between the FACSNP microarray immunoassay and ELISA: To validate the results obtained from the FACSNP microarray immunoassay with the existing "gold-standard" assay – ELISA, we performed ELISA-based measurements for the same cell medium samples (M0, M1, M2 and TAM). The ELISA-based measurements were based on the singleplex scheme. In other words, the assay targeted only one of the four cytokines in each measurement to avoid any potential crosstalk between different probe molecules. We repeated the singleplex ELISA measurements for all the four cytokines across the prepared serum samples. Finally, we compared the results generated from both methods as shown in Fig. S6. It should be noted that the measured cytokine concentrations from the FACSNP microarray immunoassay were smaller than those obtained from ELISA. This could be due to the degradation of the cytokines in the real samples during sample shipment and transportation. We believe that a side-by-side validation measurement would be ideal for probing the accuracy and reliability of the FACSNP microarray immunoassay.

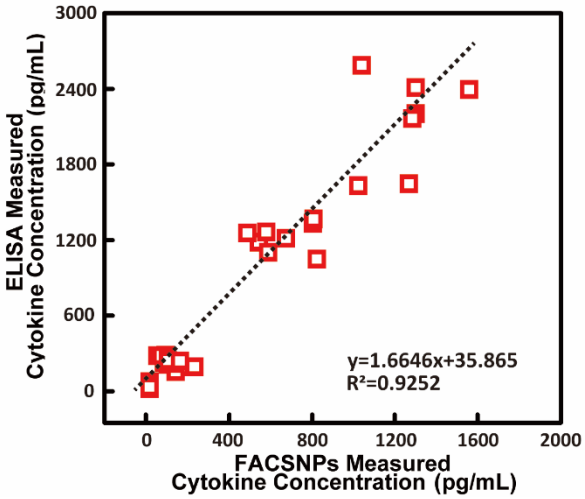

Figure S6. Correlation between results obtained from our FACSNP microarray immunoassay measurements and the ELISA for the cell medium samples.